Differences in Retinal and Choroidal Vasculature and Perfusion Related to Axial Length in Pediatric Anisomyopes

Hao Wu,[1–3] Zhu Xie,[1–3] Pengqi Wang,[1–3] Mengqi Liu,[1–3] Yuanyuan Wang,[1–3] Jiadi Zhu,[1–3] Xiangqin Chen,[1–3] Zhiqiang Xu,[1–3] Xinjie Mao,[1–3] and Xiangtian Zhou[1–4]

[1]Eye Hospital and School of Optometry and Ophthalmology, Wenzhou Medical University, Wenzhou, Zhejiang, China
[2]State Key Laboratory of Optometry, Ophthalmology and Vision Science, Wenzhou, Zhejiang, China
[3]National Clinical Research Center for Ocular Diseases, Wenzhou, Zhejiang, China
[4]Research Unit of Myopia Basic Research and Clinical Prevention and Control, Chinese Academy of Medical Sciences (2019RU025), Wenzhou, Zhejiang, China

Correspondence: Xinjie Mao, Eye Hospital and School of Optometry and Ophthalmology, Wenzhou Medical University, Wenzhou, Zhejiang, China; mxj@mail.eye.ac.cn.
Xiangtian Zhou, Eye Hospital and School of Optometry and Ophthalmology, Wenzhou Medical University, Wenzhou, Zhejiang, China; zxt@mail.eye.ac.cn.

Received: February 19, 2021
Accepted: July 2, 2021
Published: July 28, 2021

Citation: Wu H, Xie Z, Wang P, et al. Differences in retinal and choroidal vasculature and perfusion related to axial length in pediatric anisomyopes. *Invest Ophthalmol Vis Sci.* 2021;62(9):40. https://doi.org/10.1167/iovs.62.9.40

Purpose. The purpose of this study was to evaluate the interocular differences in choroidal vasculature, choriocapillaris perfusion, and retinal microvascular network, and to explore their associations with interocular asymmetry in axial lengths (ALs) in children with anisomyopia.

Methods. Refractive error, AL, and other biometric parameters were measured in 70 children with anisomyopia. Using optical coherence tomography (OCT) and OCT-angiography, we measured the submacular choroidal thickness (ChT), total choroidal area (TCA), luminal area (LA), stromal area (SA), choroidal vascularity index (CVI), choriocapillaris flow deficit (CcFD), retinal vessel density (VD), and foveal avascular zone (FAZ) area.

Results. The mean interocular differences in spherical equivalent refraction and AL were -2.26 ± 0.94 diopters and 0.95 ± 0.46 mm, respectively. Submacular ChT, TCA, LA, SA, and CVI were all significantly lower in the more myopic (longer AL) eyes than in the less myopic (shorter AL) fellow eyes. In eyes with longer ALs, both the CcFD and FAZ areas were significantly greater, whereas the superficial and deep retinal VDs were significantly less. After adjusting for corneal power and intraocular pressure, interocular differences in LA ($\beta = -0.774$), SA ($\beta = -0.991$), and CcFD ($\beta = 0.040$) were significantly associated with interocular asymmetry in AL (all $P < 0.05$).

Conclusions. In pediatric anisomyopes, eyes with longer ALs tended to have lower choroidal vascularity and choriocapillaris perfusion than the contralateral eyes with shorter ALs. Longitudinal investigations would be useful follow-ups to test for a causal role of choroidal circulation in human myopia.

Keywords: axial length, choroidal vascularity, choriocapillaris, anisomyopia, myopia

Myopia is a common visual disorder that develops primarily during childhood, when axial eye growth accelerates.[1–3] The excessive and continued ocular elongation increases the risks of developing a series of sight-threatening complications, such as macular degeneration and posterior staphylomas.[4–6] Therefore, it is essential to identify the factors responsible for ocular elongation, which are critical for myopia control.

Increasing evidence suggests that the choroid might regulate ocular growth and refractive development by modulating scleral extracellular matrix remodeling via vision-driven local signaling cascades.[7–10] Animal models of myopia have shown that choroidal thickness and choroidal blood flow are decreased in a matter of hours upon exposure to myopigenic visual stimuli, such as form-deprivation and hyperopic defocus. Such choroidal changes precede the scleral extracellular matrix remodeling and axial eye elongation that were primarily triggered by scleral hypoxia.[11–16] The role of hypoxia in the development of myopia is supported by results from studies in which choroidal blood flow was increased with the alpha adrenergic antagonist, prazosin.[17–19] Prazosin treatment inhibited the development of experimental myopia, as well as associated excessive axial elongation and scleral hypoxia.[17] This response suggests that choroidal blood flow could be predictive, prognostic, or even plays a causal role in myopia development.

Recent longitudinal studies in children have confirmed that choroidal thinning is accompanied by accelerated axial elongation during myopia development.[20–22] However, those studies lacked important information on the histophysiological status of the choroidal vasculature and choroidal blood flow. Our previous study on a small number of adult anisomyopes showed that choroidal vascularity and choriocapillaris perfusion were lower in the longer of their two

eyes.[23] Functional impairment of the retinal microvascular network was also noted in children with myopia, with decreases in vessel density and enlargement of the foveal avascular zone.[24] However, to our knowledge, no study has investigated the choroidal vasculature, choriocapillaris perfusion, and retinal microvascular network simultaneously in children with myopia. Thus, it is still unclear whether the variations in choroidal and/or retinal circulation are closely associated with longer axial length (AL) in children.

Therefore, we performed the current study in a population of children with anisomyopia, to evaluate the interocular differences in choroidal vasculature, choriocapillaris perfusion, and retinal microvascular network. Importantly, we also determined whether these variations are associated with the interocular asymmetry in ALs between the two eyes of the same individual. This approach of examining interocular differences in the same individual minimizes the confounding effects of individual variables, such as age, gender, genetics, visual environment, and diurnal rhythms, thereby allowing smaller sample sizes than typically found in population-based studies. The findings of this study will help understand the contributions of the choroidal and retinal circulations to human myopia development.

Methods

Subjects

This cross-sectional study was approved by the ethics committee of the Eye Hospital of Wenzhou Medical University. A total of 70 children, 10 to 17 years old, participated in this study; 43 were boys and 27 were girls, and the mean age was 13.1 ± 1.9 years. All participants were treated in accordance with the tenets of the Declaration of Helsinki. Written informed consents were obtained from all participants and their parents.

Ophthalmic screening examinations, including noncycloplegic subjective refraction, binocular testing, and ocular health evaluation, were conducted prior to formal enrollment. All subjects were anisomyopes with interocular difference in spherical equivalent refraction (SER) of at least 1.0 diopter (D). All subjects enrolled in the study had a best corrected visual acuity of 0.00 log minimum angle of resolution (LogMAR) or better in each eye, and there was no evidence or history of significant ocular disease, surgery, smoking, or systemic diseases. None of the subjects were previously or currently treated with myopia-control measures, such as orthokeratology or atropine; these medical histories were confirmed by their parents. Subjects were asked to avoid caffeine intake for 24 hours prior to choroidal imaging. Intraocular pressure (IOP) was evaluated by noncontact tonometry (Canon TX-20, Tokyo, Japan). Corneal power (CP) and AL were measured using the IOLMaster 700 (Carl Zeiss Meditec AG, Jena, Germany).

Swept Source Optical Coherence Tomography and Optical Coherence Tomography Angiography Imaging and Analysis

Following the screening, the participants were instructed to watch a 20-minute video on a 65-inch television (65A57F, Hisense, Shandong, China) at a distance of 5 meters, with their full-distance spectacle corrections, under normal room illumination of 200 to 300 lux. This minimized the possible influence of other recent visual experience that would induce high accommodation[25] or defocus,[26,27] which might have confounding effects on the choroid. The choroidal images were then acquired by a swept source optical coherence tomography/optical coherence tomography angiography (SS-OCT/OCTA, VG200S; SVision Imaging, Henan, China) between 9 AM and 5 PM.

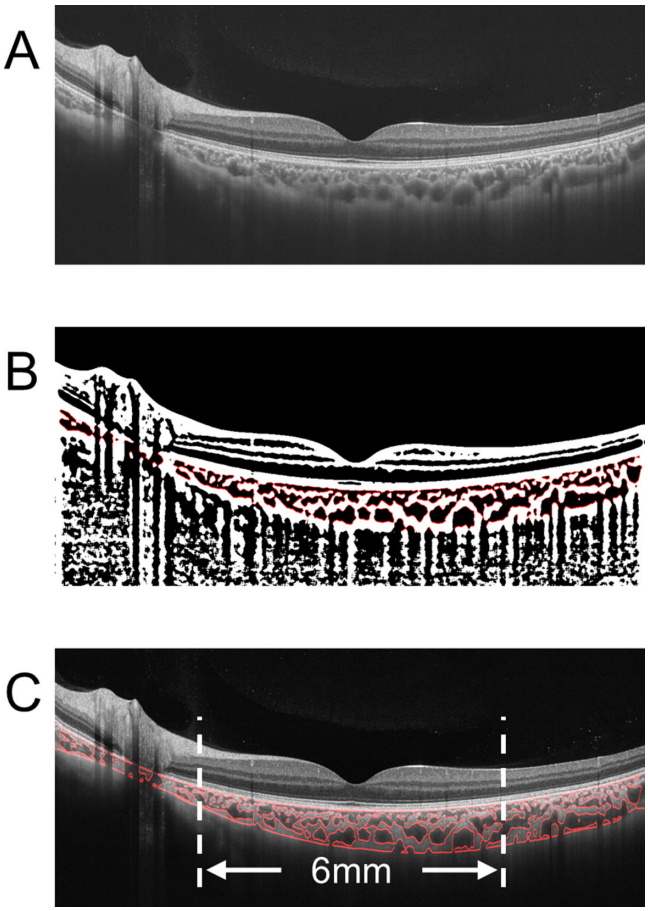

Figure 1. Choroidal image binarization. (**A**) Original OCT B-scan in horizontal meridian. (**B**) Binarized image with outline of choroidal area. (**C**) Overlay of binarized choroidal area on original image.

The SS-OCT/OCTA system contained a swept-source laser with a central wavelength of approximately 1050 nm and a scan rate of 200,000 A-scans per second. The system was equipped with an eye-tracking utility based on an integrated confocal scanning laser ophthalmoscope to eliminate eye-motion artifacts. The axial resolution, lateral resolution, and scan depth were 5 µm, 13 µm, and 3 mm, respectively.

Structural OCT imaging of the macular region was performed with 18 radial scan lines centered on the fovea. Each scan line, generated by 2048 A-scans, was 12-mm long and separated from adjacent lines by 10 degrees. Sixty-four B-scans were obtained on each scan line and were automatically averaged to improve the signal-to-noise ratio.[28] Only the vertical and horizontal lines were used to analyze the choroidal thickness and choroidal vascularity. The images were segmented semiautomatically and binarized (Fig. 1) with Niblack's autolocal threshold, using custom-designed algorithms in MATLAB R2017a (MathWorks, Natick, MA, USA), as previously described.[23] After image processing, the mean choroidal thickness (ChT), total choroidal area (TCA),

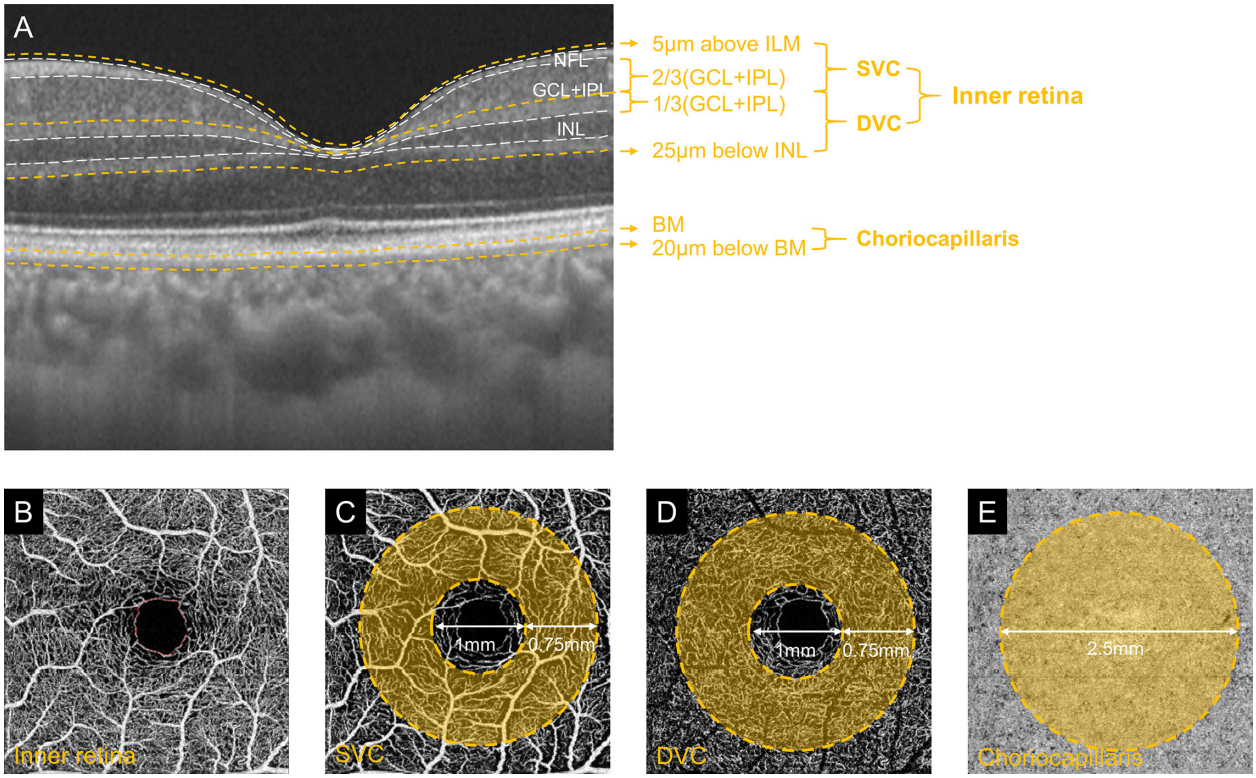

Figure 2. En face angiography for retinal vascular network and choriocapillaris layer. (**A**) Segmentation of retinal vascular layers and choriocapillaris. En face images of (**B**) inner retina with outline of FAZ, (**C**) retinal SVC, (**D**) DVC, and (**E**) choriocapillaris. Vessel density analysis in the parafoveal region for en face images of SVC and DVC, respectively. Flow deficit analysis for the choriocapillaris in the 2.5-mm submacular region. FAZ, foveal avascular zone; SVC, superficial vascular complex; DVC, deep vascular complex.

luminal area (LA), and stromal area (SA) in a 6-mm submacular region centered on the fovea were calculated. Mean ChT represented the averaged thickness measured at ca. 700 points, which were determined by the number of horizontal pixels in the 6-mm submacular region. The choroidal vascularity index (CVI) was defined as the ratio of LA to TCA.

OCTA fundus images were obtained with a raster scan protocol of 512 horizontal B-scans that covered an area of 3 × 3 mm^2 centered on the fovea. The B-scans, which contained 512 A-scans each, were repeated 8 times and averaged. The en face angiograms of inner retina, retinal superficial vascular complex (SVC), deep vascular complex (DVC), and the choriocapillaris layer (the innermost choroidal layer) were generated by automatic segmentation to evaluate retinal and choriocapillaris perfusions (Fig. 2). In the descriptions that follow, "above" and "below" refer to locations as seen in the conventional presentation of OCT images: "above" being toward the vitreous, and "below" being toward the sclera. The inner retina, containing the SVC and DVC, extended from 5 μm above the inner limiting membrane (ILM) to 25 μm below the lower border of inner nuclear layer (INL). The segmentation between the SVC and the DVC was set in the inner two-thirds and outer one-third interface of ganglion cell layer and inner plexiform layer (GCL + IPL; see Fig. 2A).[29] The choriocapillaris layer was defined as a slab from the basal border of the retinal pigment epithelium-Bruch's membrane complex to 20 μm below it.[23,30,31] The scan size was adjusted for the differences in magnification due to different ALs among the eyes.[32]

The area of the foveal avascular zone (FAZ) in the inner retina (see Fig. 2B), percentages of retinal vessel density (VD) in SVC and DVC, and percentage of choriocapillaris flow deficits (CcFD) were obtained with built-in algorithms. The percentage was calculated by dividing the area of VD or CcFD by the total area of the measured region. To reduce the influences of decentration of the fovea and artifacts at the edge of the scan, the percentages of the CcFD were calculated in a 2.5-mm diameter circular region centered on the fovea, whereas the percentage of VD was calculated in a 2.5-mm diameter annular region with 1-mm inner diameter to exclude the potential influence of the FAZ (see Figs. 2C–E).

Reproducibility of OCT and OCTA Measurements

To assess and affirm the reproducibility of OCT/OCTA measurements, 20 eyes from another 10 adults were imaged twice by an experienced observer (author Z.X.), and then the 2 sets of images were measured by the same observer at a 1-week interval. Intraclass correlation coefficients (ICCs) and coefficients of repeatability were calculated to assess reproducibility. The coefficients of repeatability were calculated as 1.96 times the standard deviation of the differences between 2 measurements. The ICCs and coefficients of repeatability generally indicated good reproducibility for both OCT and OCTA measurements (Supplementary Table S1).

Statistics

The statistical analyses were performed using SPSS Statistics 23.0 (IBM, Armonk, NY, USA). The means and standard

Investigative Ophthalmology & Visual Science

deviations of all continuous variables were calculated unless otherwise stated. Normality of the data was evaluated by the Shapiro-Wilk test. Paired *t*-tests or Wilcoxon signed-rank tests were used to assess the interocular differences between the two eyes of individuals for ocular biometrics and for retinal and choroidal parameters. Adjustment for multiple testing on these variables were not performed because of the exploratory nature of the current study.[33] Values representing the less myopic eye (with shorter AL) were subtracted from those of the more myopic eye (with longer AL) to derive interocular differences. Spearman's correlation was used to calculate the degree and statistical significance of associations between variables wherever appropriate. The multiple linear regression model with generalized estimating equations was used to determine the association between interocular differences in AL and interocular differences in those variables having a significant correlation with AL. The independent correlation matrix was set for repeated-measures of choroidal vascularity in the vertical and horizontal meridians from the same eye, and maximum likelihood estimation was specified. A value of $P < 0.05$ was considered statistically significant.

Results

Interocular Differences in SER and AL

The SER of the more myopic eyes was −2.98 ± 1.19 D, and that of the contralateral less myopic eyes was −0.72 ± 0.98 D ($P < 0.001$; Table 1). The AL in the more myopic eyes, 24.89 ± 0.93 mm, was significantly longer than that in the less myopic eyes, 23.93 ± 0.85 mm ($P < 0.001$). The interocular differences in SER and AL were −2.26 ± 0.94 D and 0.95 ± 0.46 mm, respectively, and they were strongly correlated with each other (Spearman's correlation, $r_s = -0.867$, $P < 0.001$).

Interocular Differences in Choroidal and Retinal Parameters

All 70 subjects were included in the analysis of the OCT structural B-scans, whereas 2 were excluded from the analysis for en face angiography because of poor image quality (Table 2).

Both the vertical and the horizontal mean submacular ChTs were significantly less in eyes with longer ALs than in the contralateral eyes with shorter ALs (vertical = 256 ± 55 vs. 312 ± 71 µm, horizontal = 228 ± 51 vs. 281 ± 66 µm, both $P < 0.001$). There were also significant reductions in the vertical and horizontal TCAs (vertical = 1.54 ± 0.33 vs. 1.87 ± 0.42 mm^2, horizontal = 1.37 ± 0.30 vs. 1.69 ± 0.40 mm^2), LAs (vertical = 0.89 ± 0.20 vs. 1.10 ± 0.27 mm^2, horizontal = 0.80 ± 0.19 vs. 1.00 ± 0.26 mm^2), and SAs (vertical = 0.64 ± 0.14 vs. 0.77 ± 0.17 mm^2, horizontal = 0.57 ± 0.13 vs. 0.69 ± 0.15 mm^2) in the longer eyes compared to the shorter eyes (all $P < 0.001$). Importantly, the CVIs of both the vertical and horizontal meridians were also less in the longer eyes (vertical = 58.11 ± 2.92 vs. 58.79 ± 2.46%, $P < 0.01$; horizontal = 58.07 ± 3.55 vs. 59.03 ± 2.85%, $P < 0.05$), and the percentage of CcFD was greater in the longer eyes (6.81 ± 2.77 vs. 5.23 ± 1.80%, $P < 0.001$). Moreover, the percentages of both superficial and deep retinal VD were significantly lower (superficial = 46.07 ± 3.70 vs. 46.98 ± 4.05%, deep = 56.04 ± 3.57 vs. 57.10 ± 4.20%, both $P < 0.05$), and the FAZ area was larger (0.326 ± 0.097 vs. 0.314 ± 0.099 mm^2, $P < 0.01$) in the longer eyes than in the shorter eyes.

Table 1. Ocular Biometrics of the Anisomyopic Children

Parameter	Longer Eye	Shorter Eye	Difference	*P* Value
SER (D)	−2.98 ± 1.19	−0.72 ± 0.98	−2.26 ± 0.94	<0.001†
AL (mm)	24.89 ± 0.93	23.94 ± 0.85	0.95 ± 0.46	<0.001*
CP (D)	43.38 ± 1.29	43.37 ± 1.27	0.01 ± 0.29	0.835*
IOP (mm Hg)	15.2 ± 2.9	15.1 ± 2.6	0.1 ± 2.0	0.611*

N = 70 for SER and AL, N = 69 for CP and IOP.

SER, spherical equivalent refraction; D, diopter; AL, axial length; CP, corneal power; IOP, intraocular pressure.

* *P* value determined by paired *t*-test.

† *P* value determined by Wilcoxon signed-rank test.

Table 2 Choroidal and Retinal Parameters in the Anisomyopic Children

Parameters	Longer Eye	Shorter Eye	Difference	*P* Value
ChT_V (µm)	256 ± 55	312 ± 71	−56 ± 44	<0.001*
ChT_H (µm)	228 ± 51	281 ± 66	−53 ± 47	<0.001*
TCA_V (mm^2)	1.54 ± 0.33	1.87 ± 0.42	−0.33 ± 0.27	<0.001*
TCA_H (mm^2)	1.37 ± 0.30	1.69 ± 0.40	−0.32 ± 0.28	<0.001*
LA_V (mm^2)	0.89 ± 0.20	1.10 ± 0.27	−0.21 ± 0.17	<0.001*
LA_H (mm^2)	0.80 ± 0.19	1.00 ± 0.26	−020 ± 0.19	<0.001*
SA_V (mm^2)	0.64 ± 0.14	0.77 ± 0.17	−0.13 ± 0.11	<0.001*
SA_H (mm^2)	0.57 ± 0.13	0.69 ± 0.15	−0.12 ± 0.11	<0.001*
CVI_V (%)	58.11 ± 2.92	58.79 ± 2.46	−0.68 ± 2.14	<0.01*
CVI_H (%)	58.07 ± 3.55	59.03 ± 2.85	−0.96 ± 3.26	<0.05*
CcFD (%)	6.81 ± 2.77	5.23 ± 1.80	1.58 ± 2.08	<0.001†
Superficial VD (%)	46.07 ± 3.70	46.98 ± 4.05	−0.92 ± 3.32	<0.05*
Deep VD (%)	56.04 ± 3.57	57.10 ± 4.20	−1.07 ± 3.90	<0.05*
FAZ area (mm^2)	0.326 ± 0.097	0.314 ± 0.099	0.012 ± 0.033	<0.01*

N = 70 for structural parameters; N = 68 for angiographic parameters.

_V, vertical meridian; _H, horizontal meridian. ChT, choroidal thickness; TCA, total choroidal area; LA, luminal area; SA, stromal area; CVI, choroidal vascularity index; CcFD, choriocapillaris flow deficits; VD, vessel density; FAZ, foveal avascular zone.

* *P* value determined by paired *t*-test.

† *P* value determined by Wilcoxon signed-rank test.

Choroidal Factors Associated With the Asymmetric AL

The interocular difference in AL was significantly correlated with interocular differences in most but not all choroidal parameters. The coefficients of correlation for TCA, LA, and SA ranged from −0.614 to −0.512, and for CcFD it was 0.387 (all $P < 0.01$). In contrast, AL was not correlated with the vertical or horizontal CVIs, superficial or deep retinal VD, or FAZ area (Fig. 3). In addition, the interocular differences in AL correlated significantly with that in CP ($r_s = -0.387$, $P < 0.001$) and IOP ($r_s = -0.187$, $P = 0.028$; data not shown).

The symmetry between corresponding vertical and horizontal meridians was high for interocular differences in TCA (slope = 0.890; Fig. 4A) and LA (slope = 0.962; Fig. 4B), moderate for SA (slope = 0.680; Fig. 4C), and poor for CVI (no linear relationship; Fig. 4D). To adjust the repeated-measures of the vertical and horizontal meridians, the generalized estimating equation was used to establish the multiple linear regression model and identify independent factors

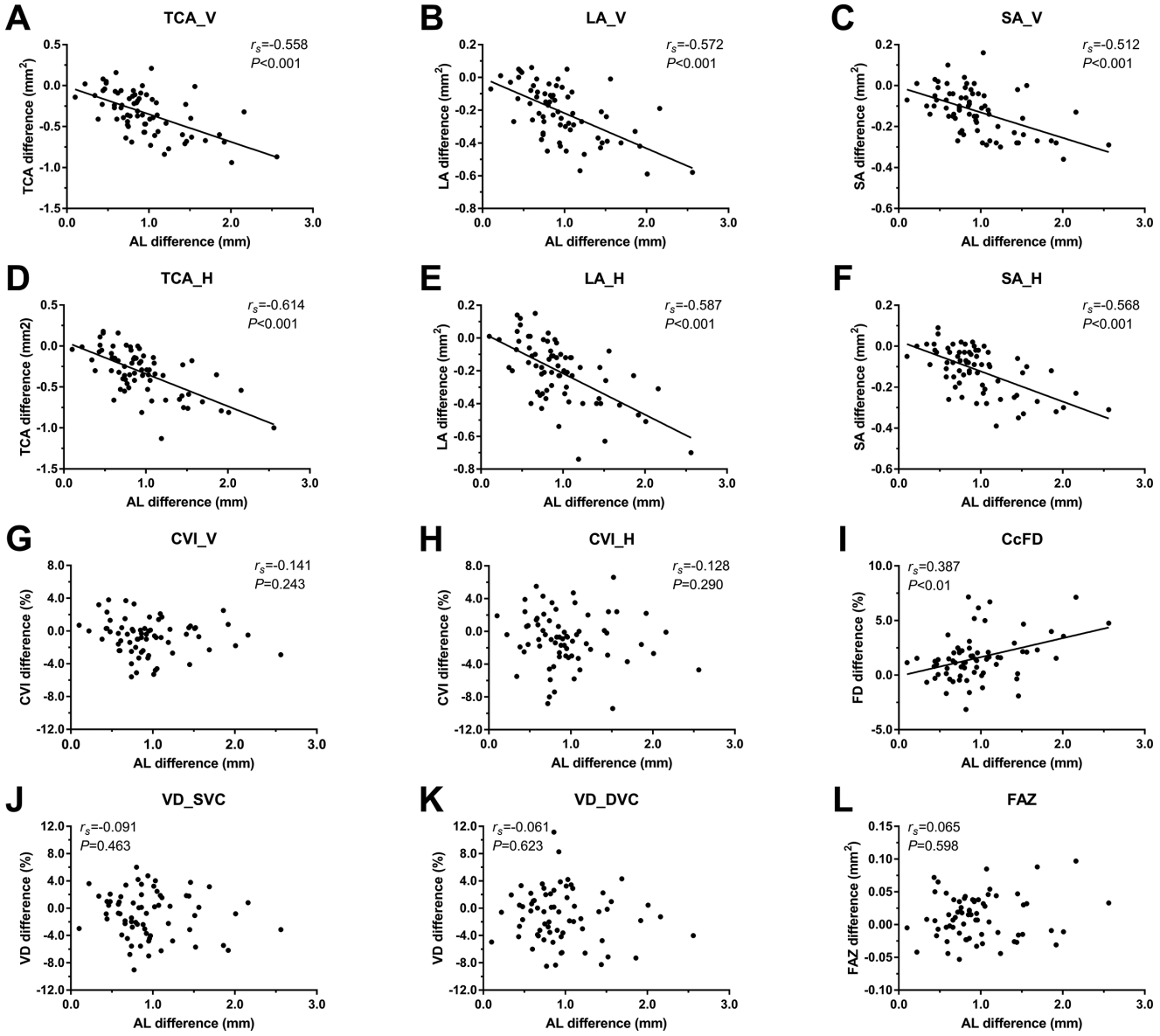

Figure 3. Correlation of interocular difference in AL with those in choroidal and retinal parameters. (**A**) TCA_V, (**B**) LA_V, (**C**) SA_V, (**D**) TCA_H, (**E**) LA_H, (**F**) SA_H, (**G**) CVI_V, (**H**) CVI_H, (**I**) CcFD, (**J**) superficial retinal VD, (**K**) deep retinal VD, and (**L**) FAZ area. Those parameters with a significant correlation with AL were fitted with a regression line. _V, vertical meridian; _H, horizontal meridian. TCA, total choroidal area; LA, luminal area; SA, stromal area; CVI, choroidal vascularity index; CcFD, choriocapillaris flow deficits; VD, vessel density; FAZ, foveal avascular zone.

that were associated with the interocular difference in AL. Because TCA included both LA and SA, these two choroidal structural parameters as well as the CcFD were included in the model (Table 3). After adjusting for CP and IOP, the interocular difference in AL was negatively correlated with the interocular differences in LA ($\beta = -0.774$) and SA ($\beta = -0.991$, both $P < 0.05$), and positively correlated with the interocular difference in CcFD ($\beta = 0.040$, $P < 0.05$).

Discussion

Excessive axial elongation is the major anatomic characteristic of myopia development, and it increases the risks for visual impairment.[34] Children who develop anisomyopia exhibit an interocular asymmetry in the magnitude or rate of axial eye growth during myopia development.[35] In the current study of pediatric anisomyopia, we found that TCA, LA, SA, CVI, and superficial and deep retinal VD were lower, whereas CcFD and retinal FAZ area were higher, in the longer eye than in the contralateral shorter eye. These findings suggest that the choroidal and retinal circulations were impaired in parallel with the excessive ocular elongation. The multiple linear regression showed that the decreases in LA and SA, as well as the increase in CcFD, were closely associated with the magnitude of ocular elongation in the longer eye.

In the past decade, cross-sectional studies have clearly shown an inverse association between AL and ChT across myopic, emmetropic, and hyperopic eyes.[36–39] Several longitudinal studies have confirmed that eyes undergoing acceler-

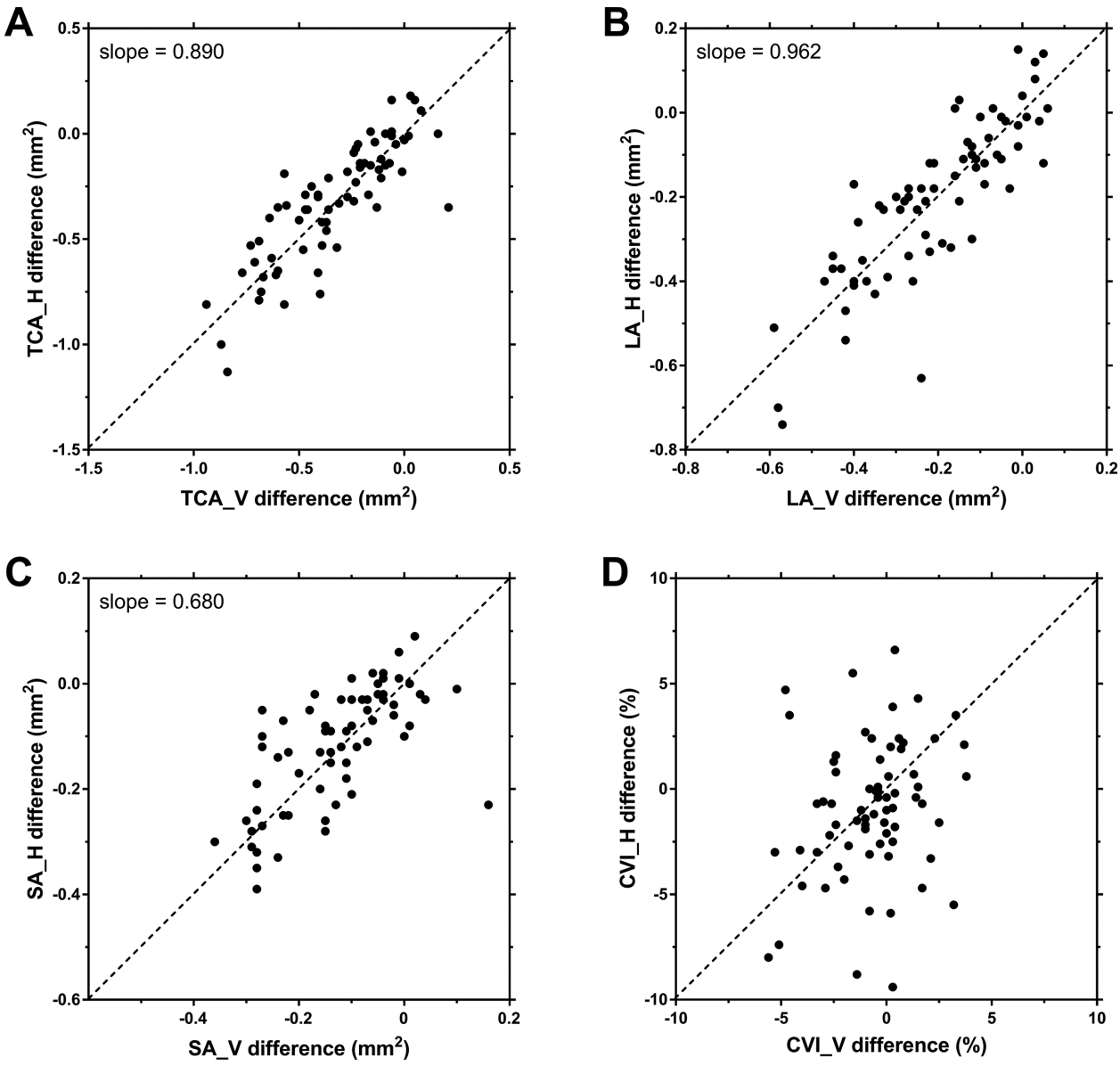

Figure 4. Scatter plots of the interocular differences in choroidal parameters at the corresponding vertical and horizontal meridians. (**A**) TCA, (**B**) LA, (**C**) SA, and (**D**) CVI. The dashed line (y = x) represents perfect symmetry between vertical (_V) and horizontal (_H) scan meridians. TCA, total choroidal area; LA, luminal area; SA, stromal area; CVI, choroidal vascularity index.

Table 3. Multiple Regression Analysis of Interocular Differences in Choroidal Parameters With the Asymmetric Axial Elongation

Variables	Unstandardized Coefficient	95% Confidence Interval	*P* Value
LA (mm²)	−0.774	−1.410 to −0.138	0.017
SA (mm²)	−0.991	−1.827 to −0.154	0.020
CcFD (%)	0.040	0.004 to 0.076	0.031
CP (D)	−0.483	−0.727 to −0.240	<0.001
IOP (mm Hg)	−0.020	−0.059 to 0.019	0.316

LA, luminal area; SA, stromal area; CcFD, choriocapillaris flow deficits; CP, corneal power; IOP, intraocular pressure.

ated ocular growth experienced less choroidal thickening or more choroidal thinning in children.[20–22] However, studies on the predictive value of ChT for axial elongation in children with emmetropia and myopia and in adults with high myopia have yielded inconsistent results. In a population-based cohort study, a thicker choroid at baseline was associated with increased 5-year axial elongation in children without myopia, whereas there was no correlation between baseline choroidal thickness and 5-year axial elongation in children with myopia.[40] Moreover, in young adults with high myopia, the presence of a thinner choroid was associated with greater axial elongation.[41] These discrepancies might

Investigative Ophthalmology & Visual Science

be attributed to variations in choroidal vascularity among subjects with different refractive states.[23,42–45] Accordingly, such variations in choroidal vascularity might in turn affect the choriocapillaris perfusion. These findings strongly imply that choroidal thickness alone is insufficient to serve as a sensitive surrogate measure of choroidal circulation. Alternatively, a detailed, comprehensive assessment of the choroidal vasculature and choriocapillaris perfusion might be more informative.[46,47]

Studies with animal models in which myopia is induced by unilateral manipulation of visual inputs have established that alteration in ChT is an early sign of vision-driven changes in ocular growth and myopia development.[13–15] The ChT responds to visual stimuli in a bidirectional, rapid, and regionally selective manner. Choroidal blood flow also exhibits a bidirectional response to visual stimuli, decreasing during myopia development and recovering after removal of the myopigenic stimuli.[11,12,48] This suggests that it might be a trigger for subsequent change in ChT and ocular growth.[15,49] Of note, our recent study in guinea pigs found that actively increasing choroidal blood flow was accompanied by attenuation of scleral hypoxia and inhibition of excessive axial elongation during form-deprivation myopia.[17] In addition, treatment with atropine, apomorphine, or intense light, all of which attenuate myopia progression, simultaneously inhibit this decrease in choroidal blood flow.[17] Overall, these provocative findings suggest that the regulation of choroidal blood flow could be a target for myopia control.

It is possible that interocular variation of choroidal circulation is a result of an active response to the differences in visual inputs between the fellow eyes. Phillips[50] reported that children with myopia who were fitted with monovision spectacles over a period of 30 months developed anisometropia. This was characterized by a slower growth rate in the near-corrected test eye than in the distance-corrected fellow eye, whereas the growth rate was reduced to the baseline level within 18 months after returning to conventional correction.[50] Such changes in ocular growth rate may be associated with retinal defocus-induced changes in the normal diurnal rhythms in ChT.[51,52] Moreover, appropriate asymmetric optical manipulations by orthokeratology were found to reduce the degree of anisomyopia in children.[53–55] It is possible that such treatments differentially affect the magnitude of choroidal thickening.[13,14] Orthokeratology treatments have been shown to increase ChT in a period as short as 3 to 4 weeks,[56–58] and this effect was sustained over the 1-year treatment period.[58] In longitudinal studies, the initial increase in ChT, mainly attributed to the thickening of the large vascular layer,[57] predicted the long-term changes in AL.[58] These findings by no means prove that the asymmetric axial elongation is the result of a vision-driven decrease in choroidal blood flow, but they certainly do indicate that this hypothesis warrants further consideration.

In agreement with the results of previous studies,[24] we also observed decreases in retinal VD and enlargement of the FAZ area in the longer eyes than in the contralateral shorter eyes in the entire study population, but these changes were not correlated with the interocular asymmetry of AL. These findings indicated that parameters of the retinal microvascular network might not be promising as predictors of axial elongation.

Both the choroid and AL undergo diurnal rhythm-associated changes,[59,60] and these circadian effects should be considered in investigations into the factors influencing the onset and progression of myopia. Under natural conditions, the diurnal rhythms of AL and ChT were reported to be similar between the two eyes of human subjects having minimal anisomyopia.[51,52] Specifically, the choroid was found to become thinner during the day and thicker during the night, approximately in anti-phase to the rhythms of the AL,[59,60] with the patterns recorded from age-matched, young adult emmetropes and myopes being not significantly different.[61–63] The choroidal LA fluctuates in parallel with the diurnal variation in ChT during the day,[64] but the CcFD are not influenced by the diurnal rhythm.[65] Even though the rhythms of AL and ChT in humans could be disturbed by exposure to about 2.00 D myopic or hyperopic defocus for 12 hours during the day, they returned to normal during the second day after removal of the lenses.[51,52] In our present study, the subjects underwent a 20-minute washout period, during which they were exposed to controlled viewing conditions while wearing full optical corrections. This approach may have helped to minimize the influence of any preceding differences in the optical defocus experiences of their two eyes.

Although our study provides clear evidence of a close association of the interocular differences in choroidal vasculature and the choriocapillaris perfusion with interocular asymmetry in AL, the cross-sectional nature of the study precludes any definite conclusions on the causality or temporal relationship. Moreover, the associations that we found were based on the analysis of interocular differences (i.e. on the degree of anisometropia rather than myopia per se). Nonetheless, this internal comparison between the two eyes of an individual allows for greater control of most systemic confounding factors. The impact of non-cycloplegic refraction on the reliability of refractive error determination was minimal, as the same technique was performed in both eyes. Additionally, most of the analyses concentrated upon the relationship between interocular choroidal variations and interocular asymmetry of ALs, which is less influenced by the lack of cycloplegia.[66] Nonetheless, it would be preferable to include cycloplegic refractions in any future longitudinal studies examining the relationship between choroidal blood flow and myopia development and progression.

Conclusions

In this study, we found a close association between the interocular differences in AL and the severity of impairment of choroidal circulation in children with anisomyopia. The interocular differences in LA, SA, and CcFD were independently associated with the interocular asymmetry in AL. These findings offer some new insight into the role of the choroid in human myopia development. Further longitudinal investigations would be highly valuable for testing the predictive value of decreased choroidal blood flow for increased ocular elongation. In this way, early interventions could be aimed at delaying the onset of myopia, rather than just slowing down the progression.

Acknowledgments

The authors thank Yue Liu (Center for Eye Disease & Development, School of Optometry, University of California, Berkeley, CA, USA) and William K. Stell (Cumming School of Medicine,

Investigative Ophthalmology & Visual Science

University of Calgary, Calgary, Alberta, Canada) for helping with the data analysis and editorial support for improving the manuscript.

Supported by the National Natural Science Foundation of China (82025009 and 82000931), National Key Research and Development Program of China (2019YFC1710204), Natural Science Foundation of Zhejiang Province (LQ21H120005), Key Research and Development Program of Zhejiang Province (2021C03053), and CAMS Innovation Fund for Medical Sciences (2019-I2M-5-048).

Disclosure: **H. Wu**, None; **Z. Xie**, None; **P. Wang**, None; **M. Liu**, None; **Y. Wang**, None; **J. Zhu**, None; **X. Chen**, None; **Z. Xu**, None; **X. Mao**, None; **X. Zhou**, None

References

1. Dolgin E. The myopia boom. *Nature.* 2015;519(7543):276–278.
2. Morgan IG, French AN, Ashby RS, et al. The epidemics of myopia: Aetiology and prevention. *Prog Retin Eye Res.* 2018;62:134–149.
3. Baird PN, Saw SM, Lanca C, et al. Myopia. *Nat Rev Dis Primers.* 2020;6(1):99.
4. Flitcroft DI. The complex interactions of retinal, optical and environmental factors in myopia aetiology. *Prog Retin Eye Res.* 2012;31(6):622–660.
5. Ohno-Matsui K, Jonas JB. Posterior staphyloma in pathologic myopia. *Prog Retin Eye Res.* 2019;70:99–109.
6. Ruiz-Medrano J, Montero JA, Flores-Moreno I, Arias L, Garcia-Layana A, Ruiz-Moreno JM. Myopic maculopathy: Current status and proposal for a new classification and grading system (ATN). *Prog Retin Eye Res.* 2019;69:80–115.
7. Wallman J, Winawer J. Homeostasis of eye growth and the question of myopia. *Neuron.* 2004;43(4):447–468.
8. Nickla DL, Wallman J. The multifunctional choroid. *Prog Retin Eye Res.* 2010;29(2):144–168.
9. Read SA, Fuss JA, Vincent SJ, Collins MJ, Alonso-Caneiro D. Choroidal changes in human myopia: insights from optical coherence tomography imaging. *Clin Exp Optom.* 2019;102(3):270–285.
10. Troilo D, Smith EL, 3rd, Nickla DL, et al. IMI - report on experimental models of emmetropization and myopia. *Invest Ophthalmol Vis Sci.* 2019;60(3):M31–M88.
11. Shih YF, Fitzgerald ME, Norton TT, Gamlin PD, Hodos W, Reiner A. Reduction in choroidal blood flow occurs in chicks wearing goggles that induce eye growth toward myopia. *Curr Eye Res.* 1993;12(3):219–227.
12. Shih YF, Fitzgerald ME, Reiner A. Choroidal blood flow is reduced in chicks with ocular enlargement induced by corneal incisions. *Curr Eye Res.* 1993;12(3):229–237.
13. Wallman J, Wildsoet C, Xu A, et al. Moving the retina: choroidal modulation of refractive state. *Vision Res.* 1995;35(1):37–50.
14. Wildsoet C, Wallman J. Choroidal and scleral mechanisms of compensation for spectacle lenses in chicks. *Vision Res.* 1995;35(9):1175–1194.
15. Zhu X, Park TW, Winawer J, Wallman J. In a matter of minutes, the eye can know which way to grow. *Invest Ophthalmol Vis Sci.* 2005;46(7):2238–2241.
16. Wu H, Chen W, Zhao F, et al. Scleral hypoxia is a target for myopia control. *Proc Natl Acad Sci USA.* 2018;115(30):E7091–E7100.
17. Zhou X, Zhang S, Zhang G, et al. Increased choroidal blood perfusion can inhibit form deprivation myopia in guinea pigs. *Invest Ophthalmol Vis Sci.* 2020;61(13):25.
18. Kiel JW, Lovell MO. Adrenergic modulation of choroidal blood flow in the rabbit. *Invest Ophthalmol Vis Sci.* 1996;37(4):673–679.
19. Kawarai M, Koss MC. Sympathetic vasoconstriction in the rat anterior choroid is mediated by alpha1-adrenoceptors. *Eur J Pharmacol.* 1998;363(1):35–40.
20. Read SA, Alonso-Caneiro D, Vincent SJ, Collins MJ. Longitudinal changes in choroidal thickness and eye growth in childhood. *Invest Ophthalmol Vis Sci.* 2015;56(5):3103–3112.
21. Jin P, Zou H, Xu X, et al. Longitudinal changes in choroidal and retinal thicknesses in children with myopic shift. *Retina (Philadelphia, PA.).* 2019;39(6):1091–1099.
22. Xiong S, He X, Zhang B, et al. Changes in choroidal thickness varied by age and refraction in children and adolescents: a 1-year longitudinal study. *Am J Ophthalmol.* 2020;213:46–56.
23. Wu H, Zhang G, Shen M, et al. Assessment of choroidal vascularity and choriocapillaris blood perfusion in anisomyopic adults by SS-OCT/OCTA. *Invest Ophthalmol Vis Sci.* 2021;62(1):8.
24. Golebiewska J, Biala-Gosek K, Czeszyk A, Hautz W. Optical coherence tomography angiography of superficial retinal vessel density and foveal avascular zone in myopic children. *PLoS One.* 2019;14(7):e0219785.
25. Woodman-Pieterse EC, Read SA, Collins MJ, Alonso-Caneiro D. Regional changes in choroidal thickness associated with accommodation. *Invest Ophthalmol Vis Sci.* 2015;56(11):6414–6422.
26. Chiang ST, Phillips JR, Backhouse S. Effect of retinal image defocus on the thickness of the human choroid. *Ophthalmic Physiol Opt.* 2015;35(4):405–413.
27. Wang D, Chun RK, Liu M, et al. Optical defocus rapidly changes choroidal thickness in schoolchildren. *PLoS One.* 2016;11(8):e0161535.
28. Alonso-Caneiro D, Read SA, Collins MJ. Speckle reduction in optical coherence tomography imaging by affine-motion image registration. *J Biomed Opt.* 2011;16(11):116027.
29. Campbell JP, Zhang M, Hwang TS, et al. Detailed vascular anatomy of the human retina by projection-resolved optical coherence tomography angiography. *Sci Rep.* 2017;7:42201.
30. Zhang Q, Zheng F, Motulsky EH, et al. A novel strategy for quantifying choriocapillaris flow voids using swept-source OCT angiography. *Invest Ophthalmol Vis Sci.* 2018;59(1):203–211.
31. Chu Z, Zhang Q, Gregori G, Rosenfeld PJ, Wang RK. Guidelines for imaging the choriocapillaris using OCT angiography. *Am J Ophthalmol.* 2021;222:92–101.
32. Dai Y, Xin C, Zhang Q, et al. Impact of ocular magnification on retinal and choriocapillaris blood flow quantification in myopia with swept-source optical coherence tomography angiography. *Quantitative Imaging in Medicine and Surgery.* 2021;11(3):948–956.
33. Bender R, Lange S. Adjusting for multiple testing–when and how? *J Clin Epidemiol.* 2001;54(4):343–349.
34. Tideman JW, Snabel MC, Tedja MS, et al. Association of axial length with risk of uncorrectable visual impairment for Europeans with myopia. *JAMA Ophthalmol.* 2016;134(12):1355–1363.
35. Vincent SJ, Collins MJ, Read SA, Carney LG. Myopic anisometropia: ocular characteristics and aetiological considerations. *Clin Exp Optom.* 2014;97(4):291–307.
36. Wei WB, Xu L, Jonas JB, et al. Subfoveal choroidal thickness: the Beijing Eye Study. *Ophthalmology.* 2013;120(1):175–180.
37. Tan CS, Cheong KX. Macular choroidal thicknesses in healthy adults–relationship with ocular and demographic factors. *Invest Ophthalmol Vis Sci.* 2014;55(10):6452–6458.

38. Read SA, Collins MJ, Vincent SJ, Alonso-Caneiro D. Choroidal thickness in myopic and nonmyopic children assessed with enhanced depth imaging optical coherence tomography. *Invest Ophthalmol Vis Sci.* 2013;54(12):7578–7586.
39. Jin P, Zou H, Zhu J, et al. Choroidal and retinal thickness in children with different refractive status measured by swept-source optical coherence tomography. *Am J Ophthalmol.* 2016;168:164–176.
40. Hansen MH, Kessel L, Li XQ, Skovgaard AM, Larsen M, Munch IC. Axial length change and its relationship with baseline choroidal thickness - a five-year longitudinal study in Danish adolescents: the CCC2000 eye study. *BMC Ophthalmol.* 2020;20(1):152.
41. Igarashi-Yokoi T, Shinohara K, Fang Y, et al. Prognostic factors for axial length elongation and posterior staphyloma in adults with high myopia: a Japanese observational study. *Am J Ophthalmol.* 2020;225:76–85.
42. Nishi T, Ueda T, Mizusawa Y, et al. Choroidal structure in children with anisohypermetropic amblyopia determined by binarization of optical coherence tomographic images. *PLoS One.* 2016;11(10):e0164672.
43. Baek J, Lee A, Chu M, Kang NY. Analysis of choroidal vascularity in children with unilateral hyperopic amblyopia. *Sci Rep.* 2019;9(1):12143.
44. Li Z, Long W, Hu Y, Zhao W, Zhang W, Yang X. Features of the choroidal structures in myopic children based on image binarization of optical coherence tomography. *Invest Ophthalmol Vis Sci.* 2020;61(4):18.
45. Gupta P, Thakku SG, Saw SM, et al. Characterization of choroidal morphologic and vascular features in young men with high myopia using spectral-domain optical coherence tomography. *Am J Ophthalmol.* 2017;177:27–33.
46. Zhou X, Ye C, Wang X, Zhou W, Reinach P, Qu J. Choroidal blood perfusion as a potential "rapid predictive index" for myopia development and progression. *Eye Vis (Lond).* 2021;8(1):1.
47. Liu Y, Wang L, Xu Y, Pang Z, Mu G. The influence of the choroid on the onset and development of myopia: from perspectives of choroidal thickness and blood flow [published online ahead of print February 7, 2021]. *Acta Ophthalmol,* https://doi.org/10.1111/aos.14773.
48. Zhang S, Zhang G, Zhou X, et al. Changes in choroidal thickness and choroidal blood perfusion in guinea pig myopia. *Invest Ophthalmol Vis Sci.* 2019;60(8):3074–3083.
49. Fitzgerald ME, Wildsoet CF, Reiner A. Temporal relationship of choroidal blood flow and thickness changes during recovery from form deprivation myopia in chicks. *Exp Eye Res.* 2002;74(5):561–570.
50. Phillips JR. Monovision slows juvenile myopia progression unilaterally. *Br J Ophthalmol.* 2005;89(9):1196–1200.
51. Chakraborty R, Read SA, Collins MJ. Monocular myopic defocus and daily changes in axial length and choroidal thickness of human eyes. *Exp Eye Res.* 2012;103:47–54.
52. Chakraborty R, Read SA, Collins MJ. Hyperopic defocus and diurnal changes in human choroid and axial length. *Optom Vis Sci.* 2013;90(11):1187–1198.
53. Chen Z, Zhou J, Qu X, Zhou X, Xue F, Shanghai Orthokeratology Study Group. Effects of orthokeratology on axial length growth in myopic anisometropes. *Cont Lens Anterior Eye.* 2018;41(3):263–266.
54. Long W, Li Z, Hu Y, Cui D, Zhai Z, Yang X. Pattern of axial length growth in children myopic anisometropes with orthokeratology treatment. *Curr Eye Res.* 2020;45(7):834–838.
55. Tsai WS, Wang JH, Chiu CJ. A comparative study of orthokeratology and low-dose atropine for the treatment of anisomyopia in children. *Sci Rep.* 2020;10(1):14176.
56. Chen Z, Xue F, Zhou J, Qu X, Zhou X. Effects of orthokeratology on choroidal thickness and axial length. *Optom Vis Sci.* 2016;93(9):1064–1071.
57. Li Z, Cui D, Hu Y, Ao S, Zeng J, Yang X. Choroidal thickness and axial length changes in myopic children treated with orthokeratology. *Cont Lens Anterior Eye.* 2017;40(6):417–423.
58. Li Z, Hu Y, Cui D, Long W, He M, Yang X. Change in subfoveal choroidal thickness secondary to orthokeratology and its cessation: a predictor for the change in axial length. *Acta Ophthalmol.* 2019;97(3):e454–e459.
59. Nickla DL. Ocular diurnal rhythms and eye growth regulation: where we are 50 years after Lauber. *Exp Eye Res.* 2013;114:25–34.
60. Chakraborty R, Ostrin LA, Nickla DL, Iuvone PM, Pardue MT, Stone RA. Circadian rhythms, refractive development, and myopia. *Ophthalmic Physiol Opt.* 2018;38(3):217–245.
61. Chakraborty R, Read SA, Collins MJ. Diurnal variations in axial length, choroidal thickness, intraocular pressure, and ocular biometrics. *Invest Ophthalmol Vis Sci.* 2011;52(8):5121–5129.
62. Burfield HJ, Patel NB, Ostrin LA. Ocular biometric diurnal rhythms in emmetropic and myopic adults. *Invest Ophthalmol Vis Sci.* 2018;59(12):5176–5187.
63. Burfield HJ, Carkeet A, Ostrin LA. Ocular and systemic diurnal rhythms in emmetropic and myopic adults. *Invest Ophthalmol Vis Sci.* 2019;60(6):2237–2247.
64. Kinoshita T, Mitamura Y, Shinomiya K, et al. Diurnal variations in luminal and stromal areas of choroid in normal eyes. *Br J Ophthalmol.* 2017;101(3):360–364.
65. Lin E, Ke M, Tan B, et al. Are choriocapillaris flow void features robust to diurnal variations? A swept-source optical coherence tomography angiography (OCTA) study. *Sci Rep.* 2020;10(1):11249.
66. Huang J, McAlinden C, Su B, et al. The effect of cycloplegia on the Lenstar and the IOLMaster biometry. *Optom Vis Sci.* 2012;89(12):1691–1696.

Investigative Ophthalmology & Visual Science